

Towards Scalable Entangled Photon Sources with Self-Assembled InAs/GaAs Quantum Dots

Jianping Wang,^{1,2} Ming Gong,³ G.-C. Guo,^{1,2} and Lixin He^{1,2,*}

¹Key Laboratory of Quantum Information, University of Science and Technology of China, Hefei 230026, China

²Synergetic Innovation Center of Quantum Information and Quantum Physics,
University of Science and Technology of China, Hefei 230026, China

³Department of Physics and Center for Quantum Coherence, The Chinese University of Hong Kong,
Shatin, New Territories, Hong Kong, China

(Received 16 December 2014; published 5 August 2015)

The biexciton cascade process in self-assembled quantum dots (QDs) provides an ideal system for realizing deterministic entangled photon-pair sources, which are essential to quantum information science. The entangled photon pairs have recently been generated in experiments after eliminating the fine-structure splitting (FSS) of excitons using a number of different methods. Thus far, however, QD-based sources of entangled photons have not been scalable because the wavelengths of QDs differ from dot to dot. Here, we propose a wavelength-tunable entangled photon emitter mounted on a three-dimensional stressor, in which the FSS and exciton energy can be tuned independently, thereby enabling photon entanglement between dissimilar QDs. We confirm these results via atomistic pseudopotential calculations. This provides a first step towards future realization of scalable entangled photon generators for quantum information applications.

DOI: 10.1103/PhysRevLett.115.067401

PACS numbers: 78.67.Hc, 42.50.-p, 73.21.La, 78.20.hb

Entangled photon pairs play a crucial role in quantum information applications, including quantum teleportation [1], quantum cryptography [2], and distributed quantum computation [3]. It has been proposed [4] that the biexciton cascade process in self-assembled quantum dots (QDs) can be used to generate “event-ready” entangled photon pairs. As shown in Fig. 1(a), a biexciton decays into two photons via two paths of different polarizations $|H\rangle$ and $|V\rangle$. If the two paths are indistinguishable, then the final result is a polarization-entangled photon-pair state [4–6] $(|H_{XX}H_X\rangle + |V_{XX}V_X\rangle)/\sqrt{2}$. However, there is a small energy difference between the $|H\rangle$ - and $|V\rangle$ -polarized photons, known as the fine-structure splitting (FSS), which is typically between approximately -40 and $+80$ μeV in InAs/GaAs QDs [7–9], much larger than the radiative linewidth (~ 1.0 μeV) [5,10]. This finite FSS leads to a time-dependent phase between the two components of the emitted two-photon state [11]. For practical use of the entangled photons, it is typically required that the FSS be as small as possible, at least smaller than the radiative linewidth [5,10]. Considerable efforts have been expended in the attempt to eliminate the FSS of excitons in QDs, and significant progress has been made in understanding [12–15] and manipulating the FSS in self-assembled QDs in recent years. Various techniques have been developed to eliminate the FSS in QDs [16–23]. In particular, it was recently found that through the application of combined uniaxial stresses or of stress in combination with an electric field, it is possible to reduce the FSS to nearly 0 for typical self-assembled InAs/GaAs QDs [23–25].

However, for the construction of practical QD devices for application in quantum information science, these devices must be scalable. One possible application of scalable entangled photon emitters, which is depicted in Fig. 1(b), is as a quantum repeater to distribute entanglement over long distances. The setup shown in Fig. 1(b) can also be used to generate multiphoton entanglement [26,27]. On-demand entangled photon emitters offer considerable great advantages of over the traditional parametric down-conversion process for the generation of multiphoton entanglement, which has a finite probability of generating more than one photon pair in an excitation cycle. In these

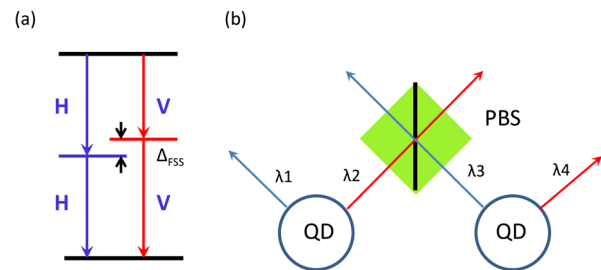


FIG. 1 (color online). (a) A schematic illustration of the biexciton cascade process. The energy difference between the H - and V -polarized photons is known as the FSS. For the preparation of entangled photon pairs, the FSS must be smaller than 1 μeV . (b) QD-based entangled photon emitters used in a quantum repeater. The entangled photon pairs from the two QDs are entangled by the polarized beam splitter, which requires that $\lambda_2 = \lambda_3$. This setup can also be used to generate multiphoton entanglement.

applications, the wavelengths of the joint photons must be identical, i.e., $\lambda_2 = \lambda_3$ in Fig. 1(b), although λ_1 and λ_4 are not necessarily equal. Moreover, it is often necessary to interface the entangled photon pairs with another quantum system, such as an N - V center, a cold atom, or another type of solid quantum system. Furthermore, because the scalability of the entangled photons strongly depends on the quality of each emitter, these applications require that the wavelengths of the QDs be tunable while maintaining the FSS at nearly 0. However, it has been found that there are strong correlations between the exciton energy and the FSS of excitons [17,28]. Furthermore, because of random alloy distributions and other uncontrollable effects, the physical properties of QDs differ dramatically from dot to dot. Therefore, it is still a great challenge to fabricate such scalable entangled photon generators using dissimilar quantum dots.

The independent tunability of the FSS and exciton energy is therefore essential for the realization of scalable entangled photon emitters. We demonstrate such tunability by proposing the application of a three-dimensional stressor to the QDs. Our basic setup is schematically illustrated in Fig. 2(a). We consider QDs that are tightly

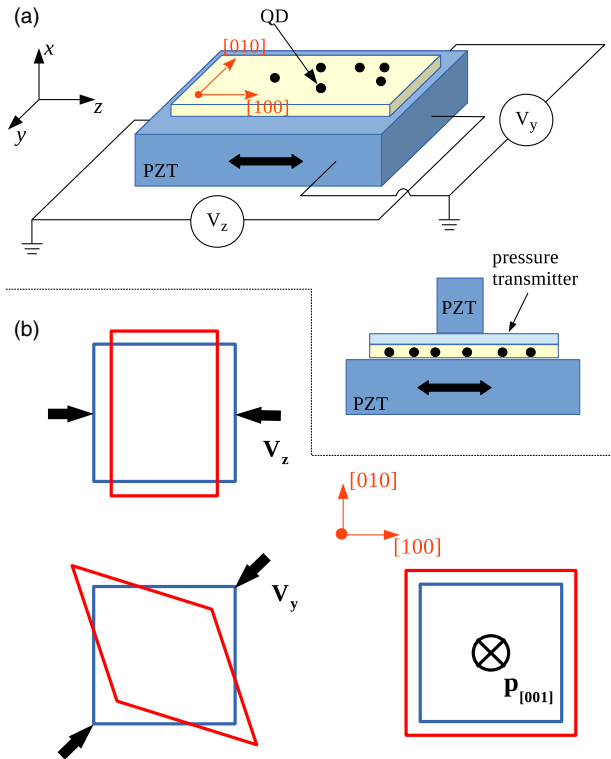


FIG. 2 (color online). (a) A three-dimensional stressor that can be used to independently tune the FSS and exciton energy in QDs. (b) Two bias voltages V_z and V_y are applied to generate in-plane strain, which is used to tune the exciton FSS. The $p_{[001]}$ stress is used to tune the exciton energy. The blue and red structures represent the shapes of the QDs before and after, respectively, the application of the voltages and stresses.

glued to the yz plane of a piezoelectric lead zirconic titanate (PZT) ceramic stack [16]. The [100] axes of the QDs samples are aligned with the polar (z) axis of PZT, whereas the [010] and [001] axes of the QDs are aligned with the y and x axes of the PZT, respectively. Two independent in-plane electric voltages V_z and V_y are applied to the PZT device as shown in Fig. 2(a), thereby generating electric fields F_z and F_y along the PZT z and y axes, respectively. The electric fields induce an in-plane strain on the QDs as follows:

$$\vec{e} = \begin{pmatrix} d_{33} & 0 & 0 \\ 0 & d_{31} & 0 \\ 0 & 0 & d_{\perp} \end{pmatrix} F_z + \begin{pmatrix} 0 & d_{15} & 0 \\ d_{15} & 0 & 0 \\ 0 & 0 & 0 \end{pmatrix} F_y, \quad (1)$$

where d_{33} , d_{31} , and d_{15} are the piezoelectric coefficients of PZT and $d_{\perp} = (d_{33} + d_{31})S_{12}/(S_{11} + S_{12})$. S_{11} , S_{12} , and S_{44} are the elastic compliance constants of GaAs. The electric fields F_z and F_y induce in-plane strains on the QDs as shown in Fig. 2(b): F_z causes strain along the [010] and [100] axes of the QD sample, whereas F_y causes strain along the [110] axis of the QDs. As demonstrated in Ref. [24], one can almost entirely eliminate the FSS in a typical InAs/GaAs QD by applying a suitable combination of such strains. To tune the exciton energy, we apply a stress along the [001] direction of the QD sample [see Fig. 2(b)], which can be achieved by placing another PZT stressor on top of the device. This pressure generates a strain e_{zz} on the QDs. To allow the photons to pass through, we can place a transparent pressure transmitter between the sample and the stressor [see Fig. 2(a)]. Now, we have a device that can freely tune the 3D strain on the QDs. Next, we will show that the device is capable of tuning the exciton emission energy over a wide range while keeping the FSS at a minimum ($< 0.1 \mu\text{eV}$).

To verify that our device functions as intended, we perform atomistic pseudopotential calculations to confirm the above predictions. We model the InAs/GaAs quantum dots by embedding InAs dots in a $60 \times 60 \times 60$ eight-atom GaAs supercell. The QDs are assumed to be grown along the [001] direction, on the top of the one monolayer InAs wetting layers [29]. To calculate the exciton energies and their FSS, we must first obtain the single-particle energy levels and wave functions by solving the Schrödinger equation

$$\left[-\frac{1}{2} \nabla^2 + V_{\text{ps}}(\mathbf{r}) \right] \psi_i(\mathbf{r}) = \epsilon_i \psi_i(\mathbf{r}), \quad (2)$$

where $V_{\text{ps}}(\mathbf{r}) = V_{\text{SO}} + \sum_n \sum_{\alpha} v_{\alpha}(\mathbf{r} - \mathbf{R}_{n,\alpha})$ is the superposition of local screened atomic pseudopotential $v_{\alpha}(\mathbf{r})$, and the total (nonlocal) spin-orbit (SO) potential V_{SO} . The atomic positions $\{\mathbf{R}_{n,\alpha}\}$ of type α at site n are obtained by minimizing the total strain energies arising from the dot-matrix lattice mismatch using the valence force field

method [30]. The pseudopotentials of the InAs/GaAs QDs are taken from Ref. [31]; these pseudopotentials have been well tested. The Schrödinger equations are solved using a linear combination of bulk bands method [32].

The exciton energies are calculated using the many-particle configuration interaction method [33], in which the (many-particle) exciton wave functions are expanded as Slater determinants for single excitons and biexcitons constructed from all of the confined single-particle electron and hole states. The exciton energy is obtained by diagonalizing the full Hamiltonian in the above basis, where the Coulomb and exchange integrals are computed numerically from the pseudopotential single-particle states, using the microscopic position-dependent dielectric constant. Including spin, this state is fourfold degenerate. The electron-hole Coulomb interactions leave this fourfold degeneracy intact. The FSS arises from the asymmetric electron-hole exchange matrix [12]. The piezoeffects are ignored in the calculation, as it was shown in Ref. [34] that the FSS of an InAs/GaAs QD changes only marginally when the piezoeffects are included.

We have calculated eight (In, Ga)As/GaAs dots. The details of structure and alloy composition for these dots are given in Table S4 of the Supplemental Material [35]. The results for two dots QD A and QD B are presented in Fig. 3(a). These results are obtained as follows: First, in the absence of $p_{[001]}$, we carefully choose the in-plane electric fields F_z and F_y to obtain the strain tensor $\vec{\epsilon}$, that reduces the exciton FSS to nearly 0 [24]. For QD A, the applied in-plane electric fields are $F_z(A) = 9.6$ kV/cm and $F_y(A) = 3.3$ kV/cm, whereas for QD B, the electric fields are $F_z(B) = 3.5$ kV/cm and $F_y(B) = 4.3$ kV/cm. We then switch on the perpendicular stress to study the evolution of the exciton energy and FSS as functions of $p_{[001]}$. Figure 3(a) depicts the exciton and biexciton emission energies for QD A and QD B as functions $p_{[001]}$ with the in-plane electric fields F_z and F_y (and thus the in-plane strain) held fixed. Although, in practice, one can apply only positive pressure (compression) to the QDs in our device, we plot the results for negative pressure simply for theoretical interest. We find that the exciton energy can be tuned over a wide range of approximately 20 meV as $p_{[001]}$ is varied from -200 to 200 MPa, with a slope of ~ 6 meV/100 MPa for both QDs. The change in exciton energy is comparable with the full width at half maximum of a general QD ensemble. These results suggest that, in principle, the exciton energies of most QDs grown in the same sample can be sufficiently tuned to become identical using our scheme. The corresponding results for the FSS are presented in Fig. 3(b). Remarkably, the change in the FSS with $p_{[001]}$ is rather small. For QD A, the FSS [the red dots in Fig. 3(b)] is approximately 0.03 μeV at $p_{[001]} = 0$. It becomes slightly larger with increasing $p_{[001]}$ and reaches ~ 0.1 μeV at $p_{[001]} = \pm 200$ MPa. The FSS of QD B [the blue squares in Fig. 3(b)] exhibits somewhat

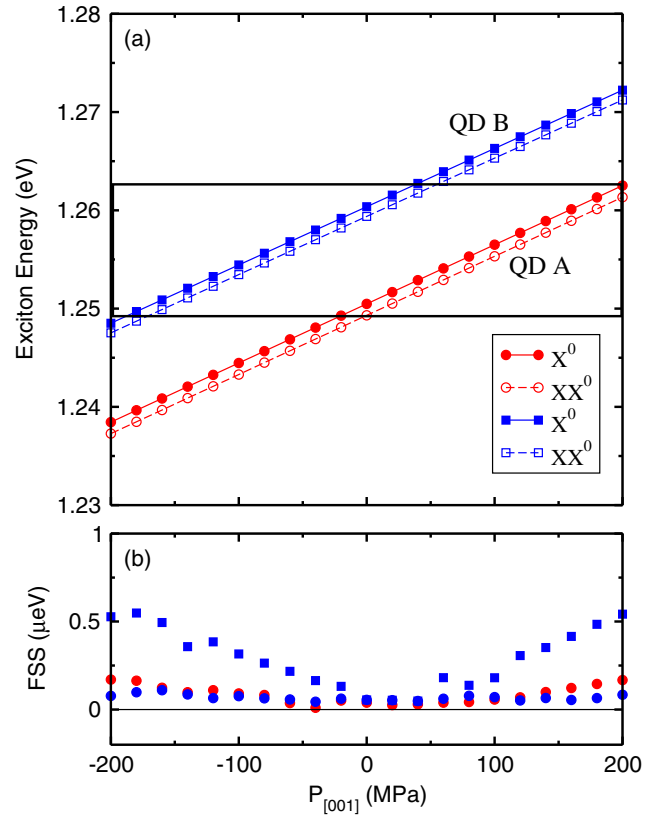


FIG. 3 (color online). (a) The exciton and biexciton energies of QD A and QD B as functions of stress $p_{[001]}$ for fixed F_z and F_y . (b) The FSSs of QD A and QD B as functions of stress $p_{[001]}$. The red dots represent the FSS of QD A for $F_z = 9.6$ kV/cm and $F_y = 3.3$ kV/cm. The blue squares represent the FSS of QD B for $F_z = 3.5$ kV/cm and $F_y = 4.3$ kV/cm, and the blue dots represent the FSS of QD B after further optimization of F_y .

stronger dependence on $p_{[001]}$ and reaches approximately 0.5 μeV at $p_{[001]} = \pm 200$ MPa. This is, nevertheless, still smaller than the homogeneous broadening of the spectrum (~ 1 μeV), which defines the upper limit on entangled photon generation. In this situation, it is possible to further reduce the FSS at a given $p_{[001]}$ by tuning the in-plane electric fields F_z and F_y . The blue dots represent the FSS of QD B after such optimization. By slightly changing $F_y(B)$ from 4.3 to 4.5 kV/cm, the FSS is reduced from approximately 0.5 μeV to approximately 0.08 μeV at $p_{[001]} = 200$ MPa. This change will shift the exciton energy by only approximately 0.02 meV. This energy shift can be compensated by increasing $p_{[001]}$ by 0.36 MPa, which causes a negligible change in the FSS. In this manner, we can tune the FSS to nearly 0 at any given exciton energy in the range within only one or two iterations. We also calculate the exciton radiative lifetimes for $p_{[001]}$. The exciton lifetimes for QD A and QD B are around 1 ns and change little with varying $p_{[001]}$, which is advantageous for the proposed device applications. We remark that the stresses applied to the samples are fairly small (< 200 MPa), on a scale that has been demonstrated

to be safe for such samples [17,20]. Specifically, it has been demonstrated that such samples are safe under hydrostatic pressure of up to 4 GPa [40].

Additional results for dots with different geometries and alloy compositions are presented in Table S5 of the Supplemental Material [35]. We fit the calculated atomic pseudopotential results using a 2×2 model [15,24]. Although it is easy to understand from the 2×2 model that, in principle, the FSS and exciton energy can be tuned simultaneously to their desired values through suitable combination of three linearly independent external fields, our scheme offers the additional advantage that the exciton energy and FSS can be tuned almost independently; i.e., the in-plane strain has a very strong effect on the FSS and a relatively small effect on the exciton energy, whereas $p_{[001]}$ has a strong effect on the exciton energy but a rather small effect on the FSS. The (nearly) independent tuning of the FSS and the exciton energy is an enormous advantage for the realization of scalable entangled photon sources. The electric field may also be used to tune the FSS [21,23]. However, the exciton energies will simultaneously change dramatically under a change in the electric field because of the Stark effects. It is therefore more difficult to tune both quantities to their target values, which requires the simultaneous tuning of the three external fields.

Now, we will consider the above results at several different levels. First, we would like to understand why in-plane strains have small effects on E_X , whereas $p_{[001]}$ has large effect? Because the envelope functions of the electron and hole states change little when the external strain is not very large, the direct electron-hole Coulomb interaction also changes little (see Fig. S1 in the Supplemental Material [35]). The change in exciton energy is therefore primarily determined by the single-particle energy gap E_g . We can estimate the slope of the relation between the exciton emission energy (or recombination energy) and the stress as follows:

$$\frac{dE(X^0)}{dp} \approx \frac{dE_g}{dp}. \quad (3)$$

If we neglect the $O(p^2)$ terms, then the slope of the change in the band gap under a variation in stress along the [001] direction can be written in accordance with the Bir-Pikus model [35]

$$\frac{dE_g}{dp} \approx -a_g(S_{11} + 2S_{12}) - b_v(S_{11} - S_{12}). \quad (4)$$

For the in-plane stresses along the [010], [100], and [110] directions, we have

$$\frac{dE_g}{dp} \approx -a_g(S_{11} + 2S_{12}) + \frac{1}{2}b_v(S_{11} - S_{12}). \quad (5)$$

Here $a_g = a_c - a_v = -6.08$ eV is the deformation potential of the band gap, and a_c and a_v are the deformation potentials

of the conduction and valence bands. $b_v = -1.8$ eV is the biaxial deformation potential of the valence bands. Because of the cancelation between the first term and the second term in Eq. (5), the in-plane stresses have a small effect on the band gap. By contrast, the stress along the [001] direction has a much larger impact on the exciton energy because the first and second terms are added.

The second question is why the in-plane stresses (strains) have a more significant influence on the FSS than does the [001] stress (strain)? Intuitively, as shown in Fig. 2(b), F_z and F_y modify the in-plane anisotropy of the QDs, whereas $p_{[001]}$ does not. The microscopic mechanism of the strain tuning of the FSS in self-assembled InAs/GaAs QDs was studied in Ref. [41], where the change in the exciton FSS under external stresses was analytically derived using the Bir-Pikus model. For simplicity, we will illustrate the results using a 6×6 model. We have

$$\Delta_{\text{FSS}} = 2|K_{\text{OD}}| \approx |2(\kappa + i\delta) + 4\varepsilon_+ K|, \quad (6)$$

where K_{OD} is the off-diagonal element of the exchange integral matrix and is equivalent to half the FSS. κ , δ , and K are exchange integrals over different orbital functions [41]. In particular, $2K \sim 300\text{--}400$ μeV is approximately the dark-bright exciton energy splitting. The exchange integrals over different orbital functions change only slightly under external strain. The change in the FSS is primarily attributable to the band mixing [41]:

$$\varepsilon_+ = \frac{R^*}{2\sqrt{3}} \left(\frac{1}{Q} + \frac{9}{\Delta} \right) + \frac{3(S^*)^2}{2Q\Delta}, \quad (7)$$

where R , Q and Δ , S are parameters in the Bir-Pikus model (see the Supplemental Material [35]). As seen from Eq. (7), Q appears only in the denominator and has a much larger value than those of R and S ; therefore, the change in ε_+ under stress primarily depends on the slopes of R and S . As shown in Table S6 of the Supplemental Material [35], the stress along the [001] direction changes only the isotropic and biaxial strains, i.e., changes only Q , and therefore has little effect on the slope of ε_+ . By contrast, the in-plane stresses modify the in-plane anisotropy of the QDs, i.e., $e_{xx} - e_{yy}$, which changes R and therefore modifies the heavy hole-light hole coupling and the FSS [35].

To conclude, we proposed a novel portable device that allows the FSS and exciton energies of (In, Ga)/GaAs QDs to be tuned (nearly) independently. This achievement represent a first step towards the future realization of scalable entangled photon-pair generators for quantum information applications, such as long-distance entanglement distribution, multiphonon entanglement, and interfaces with other quantum systems. The device can be implemented using current experimental techniques.

The authors thank C.-F. Li, J.-S. Xu, Y.-F. Huang, and B.-S. Shi for valuable discussions. L. H. acknowledges

support from the Chinese National Fundamental Research Program (2011CB921200) and the National Natural Science Funds for Distinguished Young Scholars as well as the Central Universities funding (WK2470000006). M. G. is supported by the Hong Kong RGC/GRF Projects (No. 401011 and No. 401113), University Research Grant (No. 4053072), and The Chinese University of Hong Kong (CUHK) Focused Investments Scheme.

Note added.—Recently, we became aware that Trotta *et al.* [42] have recently proposed a different device that can also tune the exciton FSS and energies independently.

*helx@ustc.edu.cn

- [1] T. Jennewein, G. Weihs, J.-W. Pan, and A. Zeilinger, *Phys. Rev. Lett.* **88**, 017903 (2001).
- [2] N. Gisin, G. Ribordy, W. Tittel, and H. Zbinden, *Rev. Mod. Phys.* **74**, 145 (2002).
- [3] J. I. Cirac, A. K. Ekert, S. F. Huelga, and C. Macchiavello, *Phys. Rev. A* **59**, 4249 (1999).
- [4] O. Benson, C. Santori, M. Pelton, and Y. Yamamoto, *Phys. Rev. Lett.* **84**, 2513 (2000).
- [5] R. M. Stevenson, R. J. Young, P. Atkinson, K. Cooper, D. A. Ritchie, and A. J. Shields, *Nature (London)* **439**, 179 (2006).
- [6] A. J. Shields, *Nat. Photonics* **1**, 215 (2007).
- [7] R. J. Young, R. M. Stevenson, A. J. Shields, P. Atkinson, K. Cooper, D. A. Ritchie, K. M. Groom, A. I. Tartakovskii, and M. S. Skolnick, *Phys. Rev. B* **72**, 113305 (2005).
- [8] A. Högele, S. Seidl, M. Kroner, K. Karrai, R. J. Warburton, B. D. Gerardot, and P. M. Petroff, *Phys. Rev. Lett.* **93**, 217401 (2004).
- [9] A. I. Tartakovskii, M. N. Makhonin, I. R. Sellers, J. Cahill, A. D. Andreev, D. M. Whittaker, J.-P. R. Wells, A. M. Fox, D. J. Mowbray, M. S. Skolnick, K. M. Groom, M. J. Steer, H. Y. Liu, and M. Hopkinson, *Phys. Rev. B* **70**, 193303 (2004).
- [10] N. Akopian, N. H. Lindner, E. Poem, Y. Berlatzky, J. Avron, D. Gershoni, B. D. Gerardot, and P. M. Petroff, *Phys. Rev. Lett.* **96**, 130501 (2006).
- [11] R. M. Stevenson, A. J. Hudson, A. J. Bennett, R. J. Young, C. A. Nicoll, D. A. Ritchie, and A. J. Shields, *Phys. Rev. Lett.* **101**, 170501 (2008).
- [12] G. Bester, S. Nair, and A. Zunger, *Phys. Rev. B* **67**, 161306 (2003).
- [13] L. He, M. Gong, C.-F. Li, G.-C. Guo, and A. Zunger, *Phys. Rev. Lett.* **101**, 157405 (2008).
- [14] R. Singh and G. Bester, *Phys. Rev. Lett.* **104**, 196803 (2010).
- [15] M. Gong, W. Zhang, G.-C. Guo, and L. He, *Phys. Rev. Lett.* **106**, 227401 (2011).
- [16] S. Seidl, M. Kroner, A. Högele, K. Karrai, R. J. Warburton, A. Badolato, and P. M. Petroff, *Appl. Phys. Lett.* **88**, 203113 (2006).
- [17] B. D. Gerardot, S. Seidl, P. A. Dalgarno, R. J. Warburton, D. Granados, J. M. Garcia, K. Kowalik, O. Krebs, K. Karrai, A. Badolato, and P. M. Petroff, *Appl. Phys. Lett.* **90**, 041101 (2007).
- [18] M. M. Vogel, S. M. Ulrich, R. Hafenbrak, P. Michler, L. Wang, A. Rastelli, and O. G. Schmidt, *Appl. Phys. Lett.* **91**, 051904 (2007).
- [19] X. M. Dou, B. Q. Sun, B. R. Wang, S. S. Ma, R. Zhou, S. S. Huang, H. Q. Ni, and Z. C. Niu, *Chin. Phys. Lett.* **25**, 1120 (2008).
- [20] F. Ding, R. Singh, J. D. Plumhof, T. Zander, V. Krapek, Y. H. Chen, M. Benyoucef, V. Zwiller, K. Dörr, G. Bester, A. Rastelli, and O. G. Schmidt, *Phys. Rev. Lett.* **104**, 067405 (2010).
- [21] A. J. Bennett, M. A. Pooley, R. M. Stevenson, M. B. Ward, R. B. Patel, A. Boyer de la Giroday, N. Sköld, I. Farrer, C. A. Nicoll, D. A. Ritchie, and A. J. Shields, *Nat. Phys.* **6**, 947 (2010).
- [22] K. D. Jöns, R. Hafenbrak, R. Singh, F. Ding, J. D. Plumhof, A. Rastelli, O. G. Schmidt, G. Bester, and P. Michler, *Phys. Rev. Lett.* **107**, 217402 (2011).
- [23] R. Trotta, E. Zallo, C. Ortix, P. Atkinson, J. D. Plumhof, J. van den Brink, A. Rastelli, and O. G. Schmidt, *Phys. Rev. Lett.* **109**, 147401 (2012).
- [24] J. Wang, M. Gong, G.-C. Guo, and L. He, *Appl. Phys. Lett.* **101**, 063114 (2012).
- [25] R. Trotta, J. S. Wildmann, E. Zallo, O. G. Schmidt, and A. Rastelli, *Nano Lett.* **14**, 3439 (2014).
- [26] J.-W. Pan, Z.-B. Chen, C.-Y. Lu, H. Weinfurter, A. Zeilinger, and M. Żukowski, *Rev. Mod. Phys.* **84**, 777 (2012).
- [27] Y.-F. Huang, B.-H. Liu, L. Peng, Y.-H. Li, L. Li, C.-F. Li, and G.-C. Guo, *Nat. Commun.* **2**, 546 (2011).
- [28] M. A. Pooley, A. J. Bennett, R. M. Stevenson, A. J. Shields, I. Farrer, and D. A. Ritchie, *Phys. Rev. Applied* **1**, 024002 (2014).
- [29] M. Gong, K. Duan, C.-F. Li, R. Magri, G. A. Narvaez, and L. He, *Phys. Rev. B* **77**, 045326 (2008).
- [30] P. N. Keating, *Phys. Rev.* **145**, 637 (1966).
- [31] A. J. Williamson, L.-W. Wang, and A. Zunger, *Phys. Rev. B* **62**, 12963 (2000).
- [32] L.-W. Wang and A. Zunger, *Phys. Rev. B* **59**, 15806 (1999).
- [33] A. Franceschetti, H. Fu, L.-W. Wang, and A. Zunger, *Phys. Rev. B* **60**, 1819 (1999).
- [34] M. Ediger, G. Bester, B. D. Gerardot, A. Badolato, P. M. Petroff, K. Karrai, A. Zunger, and R. J. Warburton, *Phys. Rev. Lett.* **98**, 036808 (2007).
- [35] See Supplemental Material at <http://link.aps.org/supplemental/10.1103/PhysRevLett.115.067401>, which includes Refs. [36–39], for parameters used in the calculations and detailed analysis of FSS under external pressure.
- [36] K. I. Kolokolov, A. M. Savin, S. D. Beneslavski, N. Y. Minina, and O. P. Hansen, *Phys. Rev. B* **59**, 7537 (1999).
- [37] http://www.efunda.com/materials/piezo/material_data/matdata_output.cfm?Material_ID=PZT-5H.
- [38] I. Vurgaftman, J. R. Meyer, and L. R. Ram-Mohan, *J. Appl. Phys.* **89**, 5815 (2001).
- [39] G. L. Bir and G. E. Pikus, *Symmetry and Strain-Induced Effects in Semiconductors* (Wiley, New York, 1974).
- [40] X. F. Wu, H. Wei, X. M. Dou, K. Ding, Y. Yu, H. Q. Ni, Z. C. Niu, Y. Ji, S. S. Li, D. S. Jiang, G.-C. Guo, L. He, and B. Q. Sun, *Europhys. Lett.* **107**, 27008 (2014).
- [41] J. Wang, G.-C. Guo, and L. He, *J. Phys. Condens. Matter* **26**, 475301 (2014).
- [42] R. Trotta, J. Martín-Sánchez, I. Daruka, C. Ortix, and A. Rastelli, *Phys. Rev. Lett.* **114**, 150502 (2015).